Available online at www.sciencedirect.com
ScienceDirect
Composite Structures 81 (2007) 21–32
COMPOSITE STRUCTURES
www.elsevier.com/locate/compstruct

Performance of externally bonded GFRP sheets on concrete in tropical environments. Part I: Structural scale tests

A. Mukherjee [a,*], S.J. Arwikar [b,1]

[a] Director, Thapar Institute of Engineering and Technology, Patiala 147004, India
[b] Department of Civil Engineering, Indian Institute of Technology, Bombay, Mumbai 400 076, India

Available online 11 January 2007

Abstract

A set of accelerated aging and natural environment tests has been carried out to evaluate performance of glass fibres reinforced polymer (GFRP) sheets bonded on concrete in tropical environment. Plain concrete beams were cast and externally reinforced by bonding with E-glass GFRP sheets. The beams were immersed in a 60 °C water bath for varying durations. The novelty of the experiment was that the environmental exposure was given while they were subjected to service loads. This load helped in keeping sheet exposed to hot water under stressed condition. Thus field environment very similar to tropical climate was simulated. The loaded specimens were also subjected to natural weathering for 6 and 12 months duration. The sheets were removed from the specimens and the tensile strength and modulus were determined to assess the degradation, if any. In the first part of the paper the structural level studies are discussed. In Part 2 the microstructural investigation is reported.

Keywords: Glass fibre reinforced polymer; Bonded sheet; Accelerated conditioning

1. Introduction

Glass fibre reinforced polymers (GFRP) sheets are being increasingly used in rehabilitation and retrofitting of concrete structures as an alternative to steel in concrete due to their high strength-to-weight ratio and corrosion and fatigue resistance. Ease of handling and application at site are added advantages. Glass fibres are of different types such as E-glass, S-2 Glass, AR-Glass, A-Glass, C-Glass, D-Glass and R-Glass depending on their properties and chemical composition. Of the different types of glass fibres, E-Glass is mostly used for reinforcement due to its high strength and electrical resistivity. Glass fibres have high strength and temperature resistance, but it is the low cost that makes GFRP the most popular FRP reinforcement in civil engineering applications. GFRPs have been found attractive in Asian region due to their cost competitiveness over carbon fibre composites [1–5].

The FRP sheets are being used for repair, strengthening and retrofitting of structural components. Degradation of steel reinforcements due to corrosion, cracking of concrete due to weathering, rapidly changing traffic needs (both in terms of intensity and load levels) and recent earthquake damages have necessitated the use of strengthening of basic structural components such as slabs, panels, walls, beams and columns [6]. Tests carried on concrete beams reinforced externally with FRP plates indicate substantial increase in the strength of the beams and decks [7–13]. Wrapping of columns with FRP have been studied for enhanced performance and are found suitable for seismic column retrofitting [14–16].

Wide spread utilization of FRPs in construction is hampered by lack of long-term durability and performance data in tropical environment [17–20]. The main environmental factors for the deterioration of GFRP are temperature, sunshine, water/moisture, alkalinity resulting from

* Corresponding author. Tel.: +91 22 2576 7343/7301/7646; fax: +91 22 2576 7302/2572 3480.
E-mail addresses: abhijit@civil.iitb.ac.in (A. Mukherjee), sjarwikar@iitb.ac.in (S.J. Arwikar).
[1] Tel.: +91 8352 262594.

0263-8223/$ - see front matter © 2006 Elsevier Ltd. All rights reserved.
doi:10.1016/j.compstruct.2006.05.013

hydration of cement in concrete and stress due to service loads. Most of the early durability tests carried out on GFRP was for applications in auto and aerospace industries. The durability data with reference to one or combinations of some of these parameters is presently available.

Beams bonded externally with GFRP sheet and subjected to wet and dry exposure under sea water resulted in 33% reduction in strength. Accelerated testing for long-term durability of GFRP laminates for marine use was done and it was found that the methodology is applicable to the plain woven cloth GFRP laminates for conventional marine use. It was characterized from the experimental results that the flexural fatigue strength of GFRP laminates decreases strongly with increasing time and temperature as well as the number of load cycles to failure [21]. The capacity of beams exposed to 100 wet/dry cycles dropped by 36%. This drop in capacity is directly related to a drop in tensile capacity of the fabric [22]. GFRPs are susceptible to alkali attack and a loss up to 100% has been reported [23]. From the review of literature it is observed that there is no standardisation of test procedures for durability of concrete-GFRP hybrid systems. The performance of such a system must be evaluated under actual environmental conditions.

The objective of the present investigation is to evaluate durability related performance parameters of one type of GFRP reinforcement sheet on concrete surface. Accelerated tests were carried out to simulate long term degradation in GFRP sheets bonded externally to plain concrete beams. The methodology of the experiments presented in this paper has been very close to the actual field conditions in tropical regions. ACI 440 recommends the test methodology for long term performance of FRP in concrete [24]. Following points along with ACI 440 were considered in the experimental study.

- The GFRP sheets are bonded on the concrete surface, as in actual structural application.
- The sheets were used as tension reinforcements in bending members as envisaged in use.
- Concrete was moist or wet as in tropical regions.
- GFRP composite sheets underwent exposure stress levels that would be seen in service.
- The synergistic effects of stress level, moisture, temperature, and alkalinity were considered.
- Elevated temperatures were used for accelerated testing. However, these temperatures did not exceed the glass transition temperature of the resin, nor were they supposed to induce any different damage condition. In the experiment the temperature was 60 °C.
- Accelerated test procedure is expected to affect the matrix and inter-phase levels, in addition to those at the fibre level.

2. Experimental program

The materials for the experimental program were procured locally wherever possible. This was to retain the regional flavour in terms of materials and in situ casting practices. Commercially available E-glass sheets and epoxy have been used for external bonding.

2.1. Concrete mix

Grade of concrete used is M35 that had a characteristic strength of 35 MPa [25]. 43 Grade ordinary Portland cement was used. No additives or plasticizers were used. Compaction was done using a table vibrator. Aggregate to cement ratio, water to cement ratio and characteristic strength is presented in Table 1.

2.2. Reinforcement characteristics

Commercially available E-glass sheets and epoxy were used for creating the sheet bonded specimens. It should be noted that the fibre volume content in the composite may vary due to the in situ bonding of the sheet on to the concrete beam. As a result, there can be variations in the property of the composite. Hence, it was considered prudent to characterize the composite by the glass fibre content only. For this purpose, effective thickness of glass fibre is calculated from the fibre volume per unit width of the sheet and the effective thickness of sheet was 0.353 mm. The design ultimate strength of the reinforcing fibre is 1500 MPa and tensile modulus is 72,000 MPa.

2.3. Specimen

The specimen consists of 100 mm wide, 100 mm deep and 1000 mm long plain concrete beams without any internal reinforcements. All the beams after casting were cured at normal temperature in a water bath for 28 days. The effective span of the beam was 940 mm. The beams were reinforced with a 20 mm wide strip of E-glass fibre sheet (Fig. 1). The strip length was adjusted to keep a gap of 25 mm between the support and the end of the strip.

Proper bonding of E-glass sheet as external reinforcement requires special technique and procedures. Concrete surface was cleaned using sand paper. Primer (epoxy of low viscosity) was applied to fill up any pores and holes and level the concrete surface. When the primer had set fully, one coat of saturant (epoxy of high viscosity) was applied on the primer coat. Then the E-glass sheet was cut to required dimension using sharp scissors. The strip

Table 1
Mix design of concrete

Mix	A/C ratio	M1	M2	FA	W/C ratio	f_c (MPa)
M35	3.9	22	40	38	0.37	38.3

A/C: aggregate to cement ratio, M1: metal (aggregate) 1, M2: metal (aggregate) 2, FA: fine aggregate, W/C: water to cement ratio, *fc*: ultimate compressive strength.

Fig. 1. 20 mm wide E-glass sheet bonded to plain concrete beam.

was wetted with the saturant and was bonded on the beam at the proper place. The strip was squeezed so that the saturant oozes out through the strip wetting all the fibres and excessive epoxy was trimmed off. After bonding the wet strip one coat of saturant was applied on top. The experimentally observed cracking moment of the beam was 0.91 kN m. The nominal moment capacity was 1.14 kN m.

2.4. Service loading

To load the beams, spring bracket-assembly was fabricated as shown in Fig. 2. The assembly consists of clamps made of steel channel sections, long threaded bolts with nuts and springs. The springs of 60 mm external diameter, 200 mm unloaded length and stiffness of 77 N mm^{-1} were used. The springs were calibrated by using a proving ring and their linearity was ensured for the entire load–deflection zone. The beams were placed back to back, with springs placed at a distance of 235 mm from the brackets. The loads were controlled by regularly monitoring the spring length while tightening the bolts.

2.5. Accelerated environmental conditioning

The beams were loaded to 20% of ultimate load as service loads. A steel tank of size 1.2 m wide, 1 m deep and 2.4 m length was fabricated to accommodate ten sets of loaded specimens at a time. The heating system was designed to maintain water at 60 ± 0.1 °C. The loaded specimens were kept in water tank for 1, 3, 6 and 9 months durations.

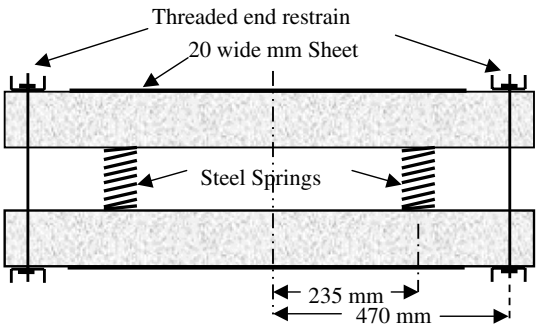

Fig. 2. Spring-bracket assembly for sustained load on E-glass sheet bonded beams.

Table 2
Designation of beams based on loading and conditioning applied

Sr. no.	Designation	Conditioning	Load position from support (mm)
1	SB0-470, SB0-350, SB0-270	SB0 → 0 months	470, 350, 270
2	SB1-470, SB1-350, SB1-270	SB1 → 1 months in tank at 60 °C	470, 350, 270
3	SB3-470, SB3-350, SB3-270	SB3 → 3 months in tank at 60 °C	470, 350, 270
4	SB6-470, SB6-350, SB6-270	SB6 → 6 months in tank at 60 °C	470, 350, 270
6	SB9-470, SB9-350, SB9-270	SB9 → 9 months in tank at 60 °C	470, 350, 270
6	ASB6-470	ASB6 → 6 months outdoor	470
7	ASB12-470, ASB12-350	ASB12 → pre-cracked 12 months outdoors	470, 350

2.6. Natural environmental conditioning

The beams were conditioned under service loads for natural weathering outdoors for 6 and 12 months duration in industrial city Mumbai (Bombay, India). The area experiences sunny weather for nine months in a year with temperatures varying from 10 to 41 °C. For three months of monsoon the area experiences one of the highest rainfalls of the country. In general the environment is typically hot and humid.

2.7. Loading scheme and designation of test beams

The loading positions have been changed progressively from the centre of the beam toward the support. Three-point loading is adopted. This was done to study the performance of beams under combined effects of bending and shear. This also simulates flexural tension in the sheet in contrast to standard pull out tests for debond. The beam section was designed to fail in compression in concrete rather than tension in the GFRP sheets. The beams were loaded at centre at a distance of 470 mm from the support of the beam. Subsequently, the load position was changed to 350 mm and 270 mm. The beams were designated as per loading position and duration of conditioning. The nomenclature is shown in Table 2.

3. Experimental results

3.1. Pilot tests

Specimens were externally bonded with 20, 30 and 40 mm wide E-glass sheets. The specimens were tested under displacement controlled universal testing machine (UTM) under four-point loading. As force to beam is transferred through the bond between sheet and concrete, the failure moments may vary significantly depending upon the bond. The rate of loading was 0.1 mm per minute. The

Table 3
Failure moments for different widths of sheets using four-point loading

Width of sheet (mm)	First crack load (kN)	Displacement at first crack (mm)	Failure load (kN)	Maximum deflection (mm)	Failure moment (kN m)
20	3.85	1.0	5.2	11.77	0.845
30	6.544	0.84	6.02	10.8	0.975
40	6.622	1.23	7.484	8.31	1.216

Table 4
Failure moment of sheet bonded beams (three-point loading)

Type of beams	Failure load (kN)	Failure moment (kN m)	Max^m deflection (mm)
SB0-470	4.5166	1.0614	0.923
SB0-350	4.7607	1.0458	2.02
SB0-230	4.5249	0.7859	0.64

results are shown in Table 3. All the beams failed due to debonding of the strip irrespective of the width of the strips. At this point it was decided to apply 20 mm wide strip on all the conditioned beams.

3.2. Failure moments

In the first set of beams at 28 days of curing, gradual loads were applied until failure. Three-point loading was applied. The support point was 30 mm from the end of the beam resulting in a moment arm of 470 mm, 350 mm and 270 mm, respectively, from the support. The failure loads, failure moments and maximum deflections are tabulated in Table 4.

3.3. Load–deflection characteristics

3.3.1. Conditioned beams

The displacements of the beams were measured using LVDTs having a travel of 25 mm and resolution of 0.01 mm. A load cell of 50 kN capacity was used to measure the loads. The load and displacement results were acquired using NIDAQ data card and transferred to computer data files. The load–deflection characteristics of the conditioned beams under three-point loading are given in Figs. 3–5.

It can be seen in Figs. 3–5 that all the original beams (SB0-470, SB0-350 & SB0-230) deflected more than the conditioned beams. The deflections were around 2 mm at failure. All fresh beams failed due to debond of the sheets. Further it can be seen that initial load–deflection behaviour of the beam is linear. The load in the beam drops significantly on the onset of the tension crack in the concrete. This points to that the GFRP sheet bridges the crack in the concrete. The stiffness of the beam declines significantly. Then after the crack width increases steadily and there is progressive slip at the GFRP concrete interface due to delamination. Ultimately the beams fail when the delamination reaches the end of the GFRP sheet. In contrast to this in all conditioned beams the GFRP sheets fractured at failure without debonding. The beams failed at higher loads but at much less deflection. The peak loads increased by 8.3%, 10.6% and 42.3% for a moment arm of 470 mm, 350 mm and 230 mm, respectively (Figs. 3–5). This is expected as the conditioned beams have much better hydration of cement due to moisture and high temperature. The ultimate deflection came down from around 2.0 mm to around 0.5 mm. One possible explanation of the increase in ultimate load and decrease in ultimate deflection is that at the onset of the tension crack the stress in the sheet was more than its strength and it could not bridge the tension crack. This also suggests that the sheets may have degraded with conditioning.

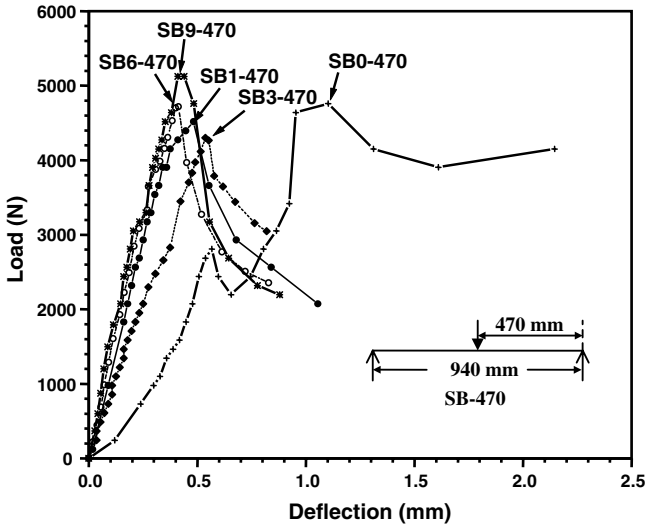

Fig. 3. Load–deflection characteristics for 470 mm moment arm (0, 1, 3, 6 and 9 months conditioned beams).

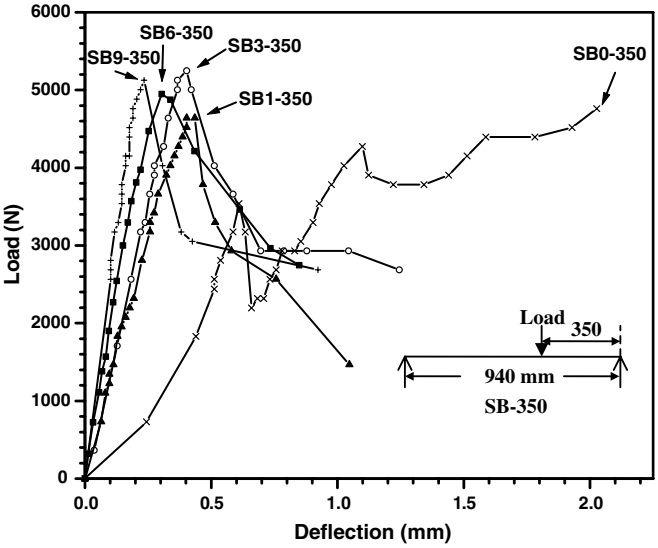

Fig. 4. Load–deflection characteristics for 350 mm moment arm (0, 1, 3, 6 and 9 months conditioned beams).

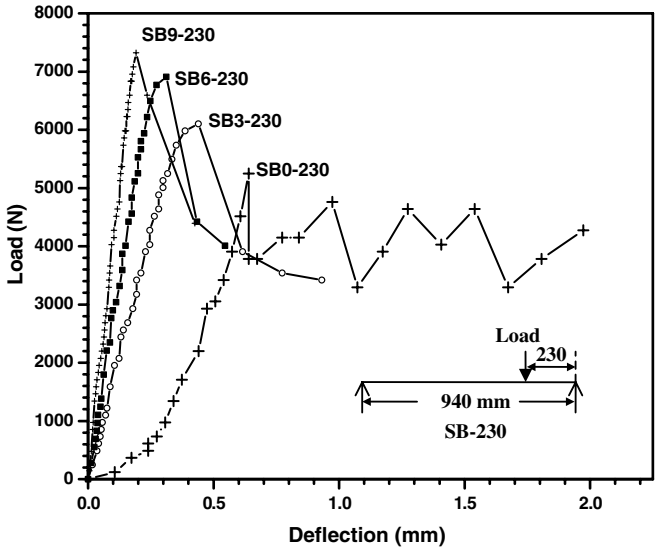

Fig. 5. Load–deflection characteristics for 230 mm moment arm (0, 3, 6 and 9 months conditioned beams).

3.3.2. Outdoor conditioned beams

A set of beams were subjected to natural weather conditioning in Mumbai. In one set a load was applied on the fresh beam until a central crack developed under the load. These pre-cracked beams were loaded to 20% of the failure load and conditioned for a year. Another set of beams were conditioned for six months without any pre-crack.

3.3.3. Uncracked specimens conditioned outdoor for six months

The beams ASB6-470 and ASB6-350, which were conditioned outdoors for six months, deflected by large amount 9.8 mm and 5 mm in comparison to 2 mm of fresh beams SB0-470 and SB0-350 (Fig. 6). The peak loads were less i.e. 37% for a moment arm of 470 mm and 20% for a moment arm of 350 mm. The reason for this reduction could be due to the development of fine thermal cracks in the plain concrete beams due to outdoor conditioning. In Fig. 6, it is seen that initial load–deflection behaviour of the beam is linear. The load in the beam drops significantly at the onset of the tension crack in the concrete. This shows that the GFRP sheet bridges the crack in concrete. Due to cracking the stiffness of the beam declines significantly. Thereafter the crack width increases steadily and there is progressive slip at the GFRP-concrete interface due to delamination. Ultimately the beams failed due to rupture of the sheets. The debonding resulted in large deflection of the beams.

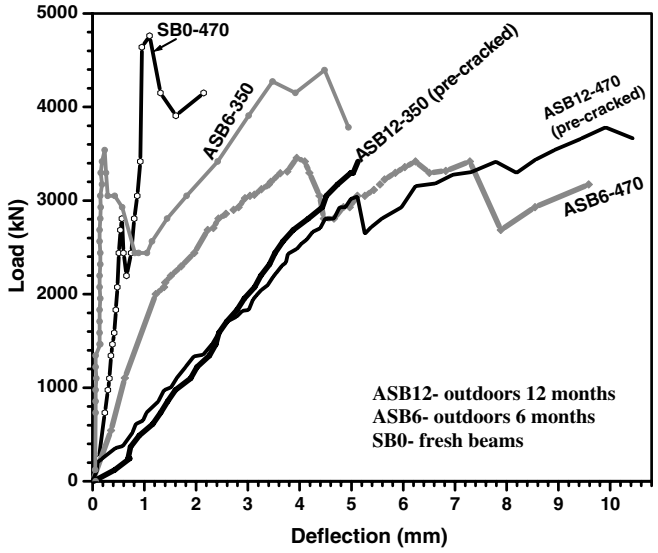

Fig. 6. Load–deflection characteristics of beams conditioned outdoors.

3.3.4. Pre-cracked specimens conditioned outdoor for 12 months

Load–deflection characteristics of pre-cracked specimens subjected to natural weathering for a year is plotted in Fig. 6. In this case, the beams were pre-cracked. The behaviour of the pre-cracked beams depends on the crack height induced and the debonding of the sheets at the time of pre-cracking. For ASB12-470, load–deflection relation was almost a straight line and the initial stiffness was much lower than the uncracked beams. The beam deflection was large due to large debond length and finally failed due to rupture of the sheets. The peak load was 41% less for a moment arm of 450 mm. For ASB12-350, the load–deflection relation was similar to beam ASB12-450 initially. The debond length was less than the earlier beam. The peak load was also 41% less for a moment arm of 350 mm. Comparison of the pre-cracked and the uncracked beams show that the difference is mainly in the initial stiffness. The ultimate load and the deflection of the beams are similar. The pre-crack did not have a pronounced effect on the environmental degradation of the specimens. The crack pattern is investigated next to understand the debonding and failure mechanism of the sheet bonded beams.

3.4. Crack pattern

The tested fresh beams, under three-point loading, are shown in Fig. 7. In the beams, at first only one crack developed under the load point as shown in Fig. 8. As load was further increased, the crack opened and failure took due to debonding of the E-glass sheet. The E-glass sheet got

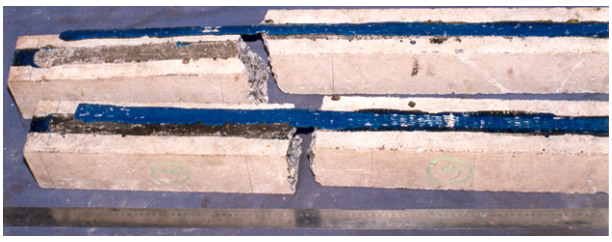

Fig. 7. Debonding in one of the broken parts of the beam due to shear failure.

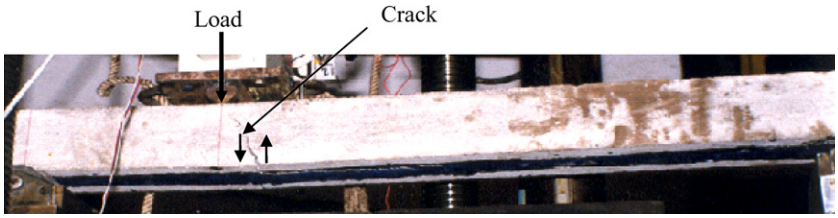

Fig. 8. Development of crack and relative displacement of the two parts of the beam due to shear under three point loading.

debonded progressively from the crack toward the support. Relative displacement of the two portions of the beam could be seen. This relative displacement abetted the stripping of the sheet. Generally stripping or peeling of the sheet took place in one of the parts of the beam (Fig. 7). Here the epoxy remained intact and concrete attached to the epoxy peeled off along the debonded interface. It can be inferred that the debond failure takes place in the concrete surface and not in the epoxy bonding the sheet composite.

In all the conditioned beams the sheets failed by rupture and no debonding was observed. The failed specimens are shown in Figs. 9 and 10. The failure of beams conditioned outdoors for 6 and 12 months took place due to partial debonding leading to the rupture of sheet (Fig. 10). The rupture of sheet suggests loss of strength of sheet due to conditioning.

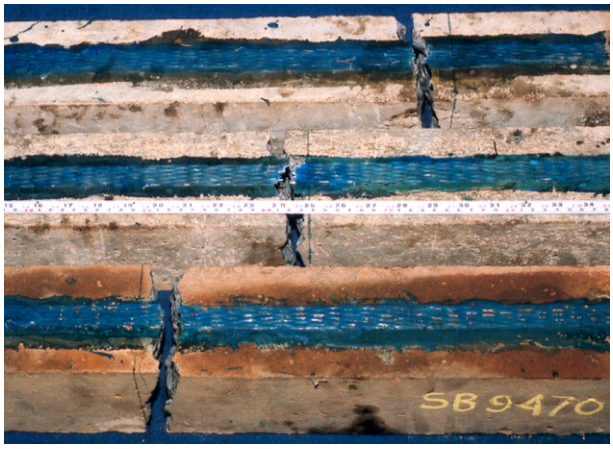

Fig. 9. Rupture of sheets conditioned for nine months (SB9-230, SB9-350 and SB9-470).

Fig. 10. Debonding and rupture of sheet for pre-cracked beams conditioned outdoors (ASB12-350 and ASB12-470).

3.5. Photoelastic investigations

In all the fresh beams only one crack formed under the load and it was observed that debond progressed from the crack towards the support. There was no edge delamination in any of the beams which was contravened to expected behaviour. To study the strain pattern at the crack and the growth of the debond photo sensitive strips were used. The method is widely used to instantly identify critical areas, highlighting overstressed and understressed regions. In this method, a special, strain-sensitive plastic coated strip is bonded to the test part. Then, as loads are applied to the beam, the coating is illuminated by polarized light from a reflection polariscope. When viewed through the polariscope, the coating displays the strains in a color fringe pattern that immediately reveals the overall strain distribution and pinpoints highly strained areas. A permanent record of the overall strain distribution was made by photographs. Photoelastic sheet of type PS-IC, item code 17000, supplied by Vishay Measurements Group was used. The fringe value of the sheet was 1850. Model 031 Basic Reflection Polariscope of the same company was used.

To find the debond length and mode of debond, the beams were pre-cracked first. This ensures that flexure modulus of concrete does not contribute to flexural strength of the concrete beam. Here only sheet contributes to the flexural strength of the beam. Four strain gauges were fixed on the sheet near the crack. Then photoelastic strip was bonded on the sheet on top of the crack. Initially, the GFRP sheet just bridges the crack and a small area around the crack is stressed. This is observed through the fringe patterns of the photoelastic strip. As the load is increased the progressive debond is sighted through the spreading of the fringes on the photoelastic sheet. The fringes for different load steps as seen through polariscope were photographed. A typical fringe pattern is shown in Fig. 11. Based on the observations through the polariscope the debonding characteristics have been plotted in Fig. 12. It can be seen that as the load is increased the debond length also increases. The maximum debond length is around 80 mm on either side of the crack. Here catastrophic debonding gets initiated and it progresses towards

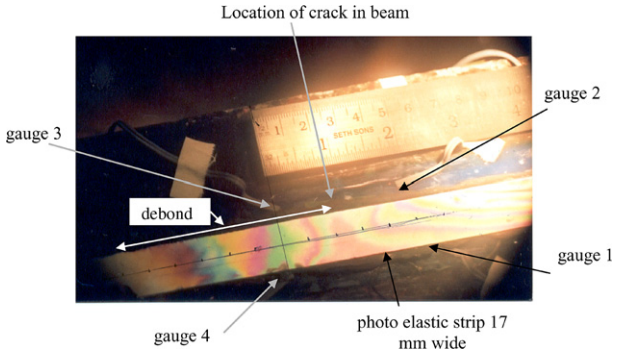

Fig. 11. Fringe patterns on photo elastic sheet at point load of 3000 N (three point loading).

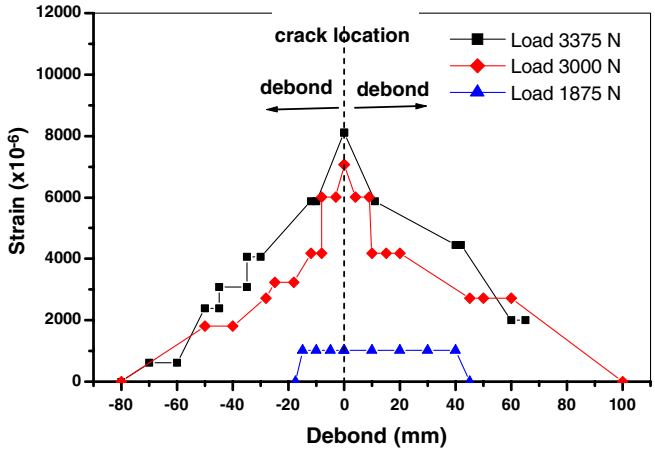

Fig. 12. Debonding characteristics of the E-glass sheet in beam, conditioned outdoors for six months.

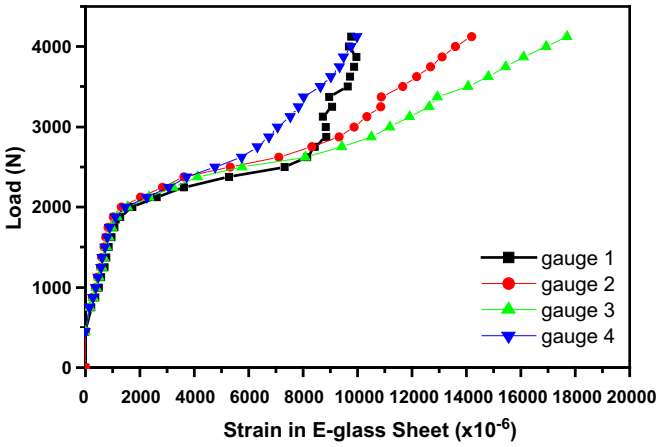

Fig. 13. Strain in E-glass sheet near the crack in the beam, conditioned outdoor for six months.

the edge of the beam leading to failure. The maximum strain in sheet at failure was about 1.77% (Fig. 13). The corresponding stress in fibre was 1275 MPa which is below the failure value of 1500 MPa. The beams fail due to debond before the stress in fibre can reach its failure value.

The highlights of the tests are:

- All conditioned beams failed at a higher ultimate load in comparison to the fresh beams.
- All conditioned beams deflected less than the fresh beams. The exceptions were beams which were weathered in natural environment. The pre-cracked beams deflected much more than uncracked beams.
- All conditioned beams failed due to rupture of GFRP sheets. All fresh beams failed due to sheet debonding.
- Debonding originated at the crack under point load and progressed towards the support progressively till failure of the beam. No edge delamination was noticed.

The different failure modes led us to the testing of the constituent materials along with the sheets to assess the property changes due to conditioning. These tests are carried out next.

3.6. Conditioned concrete

3.6.1. Compression

Twenty concrete cylinders were cast and kept in the tank at 60 °C for 1, 3, 6 and 9 months duration. The concrete was tested for the effect of accelerated aging on stress–strain behaviour [25]. The results are in Table 5. The stress–strain plot of the tested specimens is in Fig. 14. The concrete gained strength with time. The strength gain was about 22% for nine months. The ultimate strain, however, had a decreasing trend with time. The elastic constant increased with time of exposure. This is due to hydration of cement at higher temperature in presence of moisture.

3.6.2. Tension

Split tensile test was conducted on standard cylinder specimens on compression testing machine as per standards

Table 5
Effect of conditioning at 60 °C on concrete strength

Sr. no.	Duration curing	Specimen	Failure stress		Failure strain	
			Individual	Average	Individual	Average
1	28 days in water	Cylinder a	32.82	31.68	0.00158	.00189
		Cylinder b	31.689		0.002	
		Cylinder c	30.55		0.00208	
2	One month at 60 °C	Cylinder a	31.689	33.95	0.0018	.00171
		Cylinder b	35.08		0.00187	
		Cylinder c	35.08		0.00147	
3	Three months at 60 °C	Cylinder a	35.085	37.38	0.00128	.00132
		Cylinder b	37.45		.00135	
		Cylinder c	39.61		.00132	
4	Six months at 60 °C	Cylinder a	32.82	35.08	0.00131	.00135
		Cylinder b	36.21		0.00139	
		Cylinder c	36.21		0.00135	
5	Nine months at 60 °C	Cylinder a	37.35	38.48	0.00128	.00133
		Cylinder b	38.48		0.00131	
		Cylinder c	39.61		0.0014	

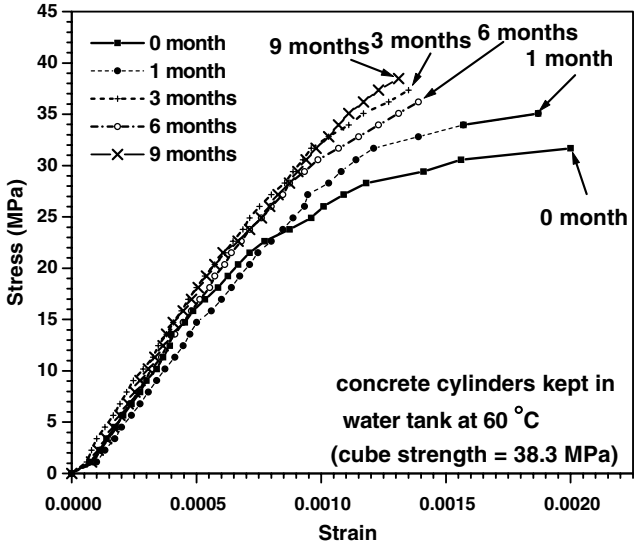

Fig. 14. Stress vs. strain plot of concrete cylinders conditioned in water tank at 60 °C.

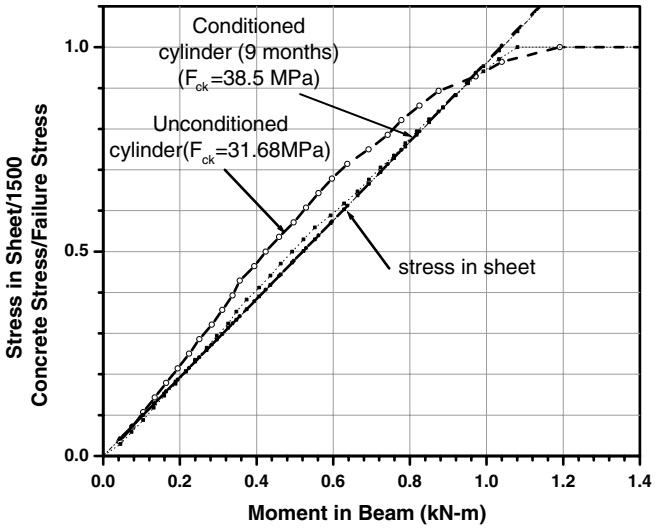

Fig. 15. Stresses in concrete and sheet corresponding to the moment in the beam.

Table 6
Spilt tensile strength of concrete

Sr. no.	Sample description	Tensile strength f_t (MPa)	Percentage change
1	Cylinder at 28 days	2.037	–
2	Cylinder conditioned for nine months in tank at 60 °C	3.763	+84.7

[26–28]. Line load on the cylinder specimen in horizontal position was applied and the failure load at which the cylinder split into two halves about the vertical diametrical plane was noted. The test was repeated for three specimens and the average tensile strength has been calculated and recorded in Table 6. There is 85% increase in tensile strength of concrete in nine months due to accelerated ageing. It is expected that flexural modulus of concrete will also increase in the same proportion.

The increase in failure load capacity of the conditioned beams may be due to the increase in the capacities in the concrete. However, our focus is in the condition of the sheets. Although there have been increase in load capacities of the beam there has been a marked difference in the failure modes in the beams. While the fresh beams failed due to debonding of sheet the conditions beams failed due to their rupture. To investigate this point the sheet forces were estimated using a numerical model.

4. Numerical model and results

Based on the experimentally observed stress–strain behaviour of concrete and GFRP sheet a numerical model is developed to estimate the stresses in concrete and GFRP at different load levels [29]. Following assumptions have been made:

- Strain varies linearly along the depth of the beam.
- The tensile strength/flexural modulus of the concrete is negligible.

With these assumptions the neutral plane depth can be calculated by applying the conditions of equilibrium along the axis of the beam. Stress–strain relationships of the conditioned and unconditioned cylinders in Fig. 14 are used to evaluate stresses in concrete and rebar at any stage of loading in the specimen section. The maximum plastic strain in concrete assumed is 0.0035. The resultant bending moment is calculated by applying moment equilibrium condition.

The unconditioned beam SB0-470 failed at 1.06 kN m due to debond. Both the compressive stress in concrete and the stress in the sheet reached about 95% of its ultimate failure value (Fig. 15). The conditioned beam SB9-470 failed at 1.2 kN m. The stress in the sheet exceeds its design ultimate strength. The rupture of the sheet is justified here. However, SB3-470 and SB6-470 failed in rupture of sheet when the stress in sheet was only 95% of its design ultimate strength. The sheets did not debond and they ruptured instead. At this point it was decided to investigate the sheets by removing them from the conditioned beams.

5. Test of conditioned sheet composite

The E-glass sheets were removed from the conditioned beams and were investigated for their material properties like tensile strength and modulus of elasticity. Care was taken to avoid any damage to the sheets. The sheet specimens were cut out in length, to suit the holding mechanism of universal testing machine (UTM). The GFRP sheets are weak in shear and fail at the grips in UTM. End grips were prepared for sheet tensile testing by attaching extra E-glass sheet with epoxy at the ends [30]. The prepared specimen with the extensometer is shown Fig. 16.

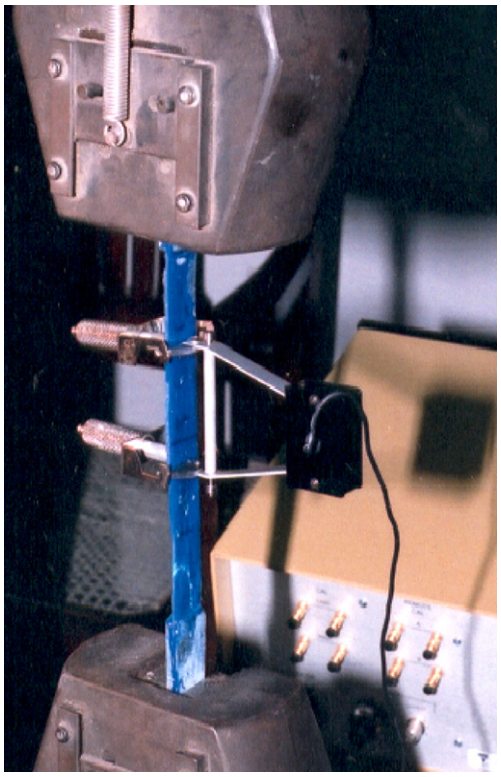

Fig. 16. E-glass strip with clamp type extensometer.

The results of the tensile tests are tabulated in Table 7. The stresses in the sheet fibre are calculated assuming that the strain in fibre and epoxy are same. Due to accelerated ageing the GFRP sheets lost their strength by 13.9%, 20.3%, 33.25% and 36.16% in 1, 3, 6, and 9 months of conditioning. The reduction in strength of E-glass fibres due to conditioning is plotted in Fig. 18. It is of exponential nature with time. The sheets conditioned outdoor for six months surprisingly increased in strength by 30%. However, the increase in 12 months of outdoor conditioning was only 6%. This could be due to cross-linking phenomenon in the epoxy resulting in increase in its strength and through better shear transfer between fibre and epoxy.

Table 7
Comparative study of properties of conditioned GFRP composite sheet

Sr. no.	Sample	Conditioning	Exposure duration (months)	Tensile stress in fibre at failure	
				Mean (MPa)	% Change
1	Bare strip 20 mm	–	–	772	–
2	Sheet composite	–	–	794.2	–
3	Sheet composite	Tank at 60 °C	1	683.6	−13.9
4	Sheet composite	Tank at 60 °C	3	632.8	−20.32
5	Sheet composite	Tank at 60 °C	6	530.15	−33.25
6	Sheet composite	Tank at 60 °C	9	507.03	−36.16
7	Sheet composite	Outdoor	6	1028.44	+29.49
8	Sheet composite	Outdoor	12	841.79	+5.99

The behaviour of composite depends upon the percentage of fibre in epoxy. The epoxy is 2 mm average thick and 20 mm wide with modulus of elasticity as 3.034 GPa. The sheet is 0.353 mm thick and 20 mm wide with modulus of elasticity as 72.4 GPa. The modulus of elasticity of the

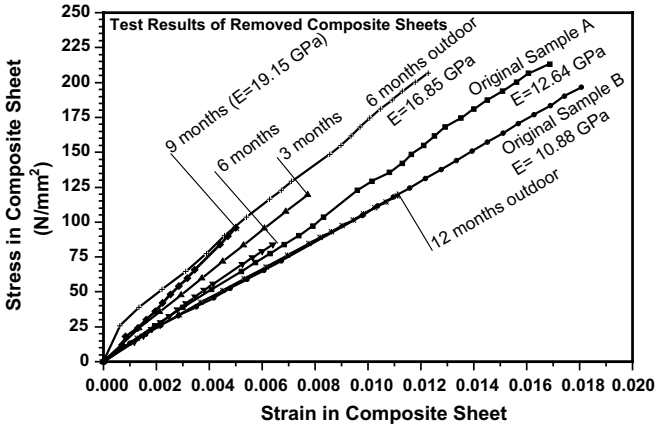

Fig. 17. Stress–strain diagram of conditioned composite sheets.

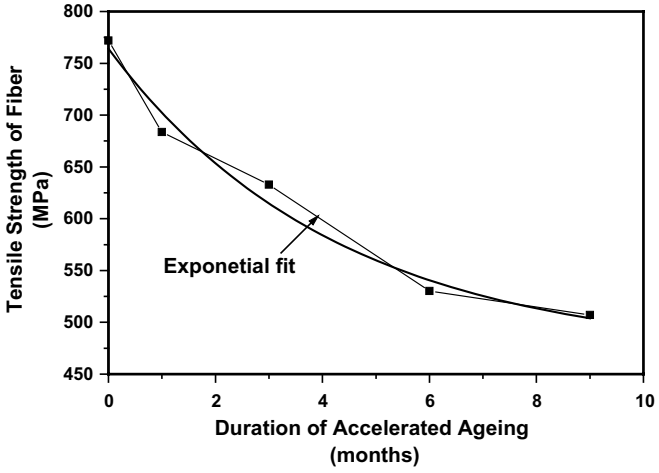

Fig. 18. Decrease in strength of GFRP sheet fibre due to accelerated ageing.

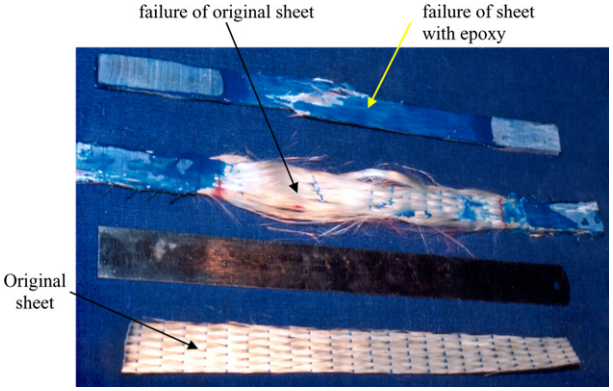

Fig. 19. The failure of original E-glass sheet with and without epoxy.

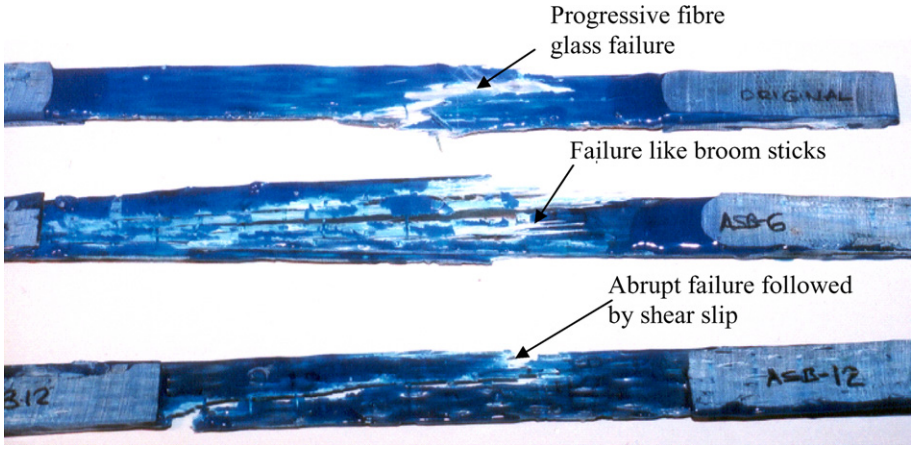

Fig. 20. Comparison of failure of original E-glass sheet with conditioned sheets in air for six months (ASB-6) and 12 months (ASB-12).

composite sheet works out to be 15.6 GPa based on fibre volume fraction. From stress–strain diagram of tested sheets (Fig. 17) it can be seen that the modulus of elasticity of the sheets varied from 10.88 to 19.15 GPa. Here, the stresses are calculated on the basis of net composite sectional area. These variations can be attributed to the variations in the epoxy thickness, error in cutting exact 20 mm wide woven sheet, changes in properties of the constituent materials due to conditioning and mode of failure of sheet composite.

The original sheet failed due to individual fibre rupture. It is very rare that all the fibres fail at a time across the cross-section. The fibre failure produced a snapping sound. The failed specimens are shown in Fig. 19. All the sheets have been tested at room temperature of about 25 °C. Two samples A and B were tested after curing them for 7 days and 2 days (Fig. 20) and modulus of elasticity obtained was 12.64 and 10.88 GPa. The curing of the epoxy increases the strength and the stiffness of the sheet at the early stages. The comparison of failure of sheets conditioned in air is shown in Fig. 20. The sheet conditioned for six months outdoors failed in a typical broom shape while 12 months outdoor specimens failed abruptly without any warning. The comparison of failure of conditioned sheets is shown in Fig. 21. Here at failure no warning of any sort such as snapping of individual fibres or excessive deformation could be observed.

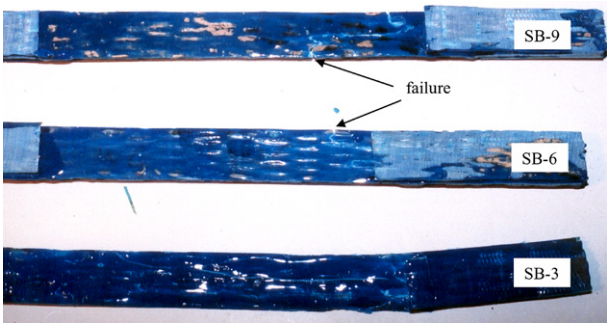

Fig. 21. Comparison of failure of E-glass sheet conditioned in tank for 3 months (SB-3), 6 months (SB-6) and 9 months (SB-9).

6. Durability of GFRP sheets

The durability of the E-glass sheet was studied based on results available. The effect of conditioning on epoxy strength is neglected for calculation of the stresses in the fibre. The strength of the fibre due to accelerated ageing is plotted in Fig. 22. The outdoor result of 12 months could not be interpolated from the formula given in Fig. 22 as there was no degradation in tensile strength [19]. Results with 20–30% reduction in strength due to outdoor conditioning are required. This would require outdoor results with more time of exposure. The sheets did not degrade as the fibres were protected with relatively thicker epoxy coating of about 1.547 mm. The sheets with thicker coating are expected to last longer in the field.

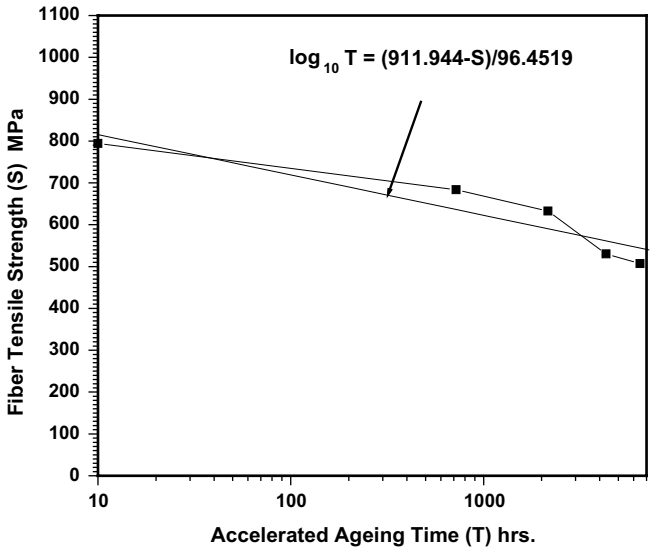

Fig. 22. Effect of accelerated ageing on tensile strength of sheet.

7. Summary and conclusion

The primary aim of the investigation was performance of externally bonded GFRP sheets on concrete. All the fresh/test beams behaved on expected lines i.e. final failure took place due to debond of the sheets and the sheets remained in tact. Only one crack developed under the load under the three-point loading and this crack was bridged by the composite sheet until debond took place. However, mode of failure of the beams changed after they were conditioned under simulated tropical climate. All conditioned beams withstood higher loads than the fresh beams. The increase was around 13.5% in nine months of conditioning in water tank at 60 °C. The beams conditioned outdoors (pre-cracked) for 12 months failed at a lesser load but deflected more than the fresh beams primarily due to debond. The decrease in failure load was 18.9% while the increase in deflection was large at 370%. The average stiffness of the beam was variable. However, all beams showed increase in stiffness due to conditioning. But there was a marked change in the failure mode. In contrast to debond of fresh beams the conditioned beams failed due to rupture of the composite sheets. The failure strain of the sheet is 2%. The strain in composite sheet bonded to fresh beams varied from 0.8% to 1.2% as it debonded before failure. The strains at failure in the pre-cracked beams, conditioned six months outdoor, varied from 1.0% to 1.8%. None of the beams had edge de-lamination.

The test of constituent materials showed that the concrete gained substantial strength due to conditioning in tank at 60 °C. The compressive strength increased by 22%. The split tensile strength increased by 85%. The elastic modulus increased by 21%. This is primarily due to accelerated hydration of cement in concrete due to moisture and temperature. The sheets removed from the conditioned beams revealed that GFRP sheets lost their strength by 13.9%, 20.32%, 33.25% and 36.16% in 1, 3, 6 and 9 months of accelerated conditioning. Surprisingly the sheet gained strength due to conditioning outdoors. The increase in 6 and 9 months was 29.49% and 6%. This could be due to increase in the strength of epoxy due to cross-linking of bonds in the epoxy. The epoxy in the sheet conditioned for nine months absorbed moisture in a short time. This indicated that the epoxy had degraded due to conditioning.

There was a large variation in modulus of elasticity from 10.88 to 19.16 GPa in the tested composite sheets. This is mainly because the constituent materials have largely varying modulus of elasticity and percentage of area. The modulus of elasticity of E-glass sheet and epoxy used are 72.4 GPa and 3 GPa. The modulus of the composite sheet depends on the thickness of the epoxy and the amount of fibre in it. Based on the fibre volume content the calculated value is 15.59 GPa. The thickness of epoxy depends on how the coat is applied and amount of fibre depends on the accuracy of cutting the 20 mm strip from the woven sheet.

Despite thick layer of around 1.65 mm epoxy over the 0.353 thick sheets, the sheets degraded substantially due synergistic effect of heat, moisture, stress and alkali. However, it appears that epoxy protected the fibres under natural environment as the strength did not decrease even after one year of outdoor conditioning. As there was no degradation in the strength within one year of natural conditioning, extrapolating the field life of sheets was not possible. This requires conditioning of beams outdoors for more time. The methodology can be used to predict the long-term behaviour of GFRP sheet bonded to concrete beams in terms of years. More tests with different temperatures, alkalinity and pre-stressing stresses are required to build model to predict the rate and quantum of damage to the fibres.

The dual effect of increase in strength of concrete and decrease in strength of the sheet is the cause of changes in the failure mode of conditioned beams. Due to the increase in the strength of concrete the failure loads were higher in the conditioned beams. The stiffness of the sheet did not change appreciably. As a result, the stiffness of the beam went up. The strength of the sheet, on the other hand, reduced considerably. This led to the shift in failure mode from sheet debond to sheet rupture. The causes of degradation of the sheets have been investigated through microstructural studies. The results of this study are presented in Part 2.

Acknowledgements

The authors acknowledge Prof. C.E. Bakis, Dept. of Engg. Science and Mechanics and Prof. T.E. Boothby, Dept. of Architectural Engineering, Pennsylvania State University, USA, for their contribution in formulating the test matrix and valuable suggestions. The financial support for this research was received from National Science Foundation, USA and Department of Science and Technology, India. Ms. Tennisha Brown of Pennsylvania State University helped in conducting the photoelastic experiments at I.I.T. Bombay.

References

[1] Nanni A. Fiber-reinforced-plastic (FRP) reinforcement for concrete structures: properties and applications. Elsevier Science Publishers B.V.; 1993.
[2] Saadatmanesh H. Fiber composites for new and existing structure. ACI Struct J 1994;91(3):346–54.
[3] Mohr JG, Rowe WP. Fiber glass. New York: Van Nostrand Reinhold; 1978.
[4] Holmes M, Just DJ. GRP in structural engineering. New York: Applied Science Publishers; 1983.
[5] Karbhari VM. Material considerations in FRP rehabilitation of concrete structures. J Mater Civil Eng 2001;13(2):90–7.
[6] Karbhari VM, Zhao L. Use of composites for 21st century civil infrastructure. Comput Meth Appl Mech Eng 2000;185:433–54.
[7] Wang YC, Chen CH. Analytical study on reinforced concrete beams strengthened for flexure and shear with composite plates. J Compos Struct 2003;59:137–48.
[8] Arduini M, Nanni A. Parametric study of beams with externally bonded FRP reinforcement. ACI Struct J 1997;94(5):493–501.

[9] Malek AM, Saadatmanesh H, Ehasani MR. Prediction of failure load of R/C beams strengthened with FRP plate due to stress concentration at the plate end. ACI Struct J 1998;95(1):142–52.
[10] Kachlakeva D, McCurry DD. Behaviour of full-scale reinforced concrete beams retrofitted for shear and flexural with FRP laminates. Compos Part B 2000;31:445–52.
[11] Sim J, Oh H. Structural improvement of strengthened deck panels with externally bonded plates. Cement Concrete Res 2005;35: 1420–9.
[12] Tenga JG, Caob SY, Lama L. Behaviour of GFRP-strengthened RC cantilever slabs. Constr Build Mater 2001;15:339–49.
[13] Saadatmanesh H, Malek AM. Design guidelines for flexural strengthening of RC beams with FRP plates. J Compos Constr ASCE 1998;2(4):158–64.
[14] Parvin A, Jamwal AS. Performance of externally FRP reinforced columns for changes in angle and thickness of the wrap and concrete strength. J Compos Struct 2006;73:451–7.
[15] Mukherjee A, Joshi MV. Seismic retrofitting using fibre composites. Indian Concrete J 2002;76(8):496–502.
[16] Rochette P, Labossiere P. Axial testing of rectangular column models confined with composites. J Compos Constr ASCE 2000;4(3):129–36.
[17] Hulatt J, Hollaway L, Thorne A. Preliminary investigations on the environmental effects on new heavyweight fabrics for use in civil engineering. Compos Part B 2002;33:407–14.
[18] Marsh G. Durability—a key issue for composites in infrastructure. Reinforced Plastics 1997(July/August):26–30.
[19] Mukherjee A, Arwikar SJ. Performance of glass fiber reinforced polymer reinforcing bars in tropical environments—Part I: structural scale tests. ACI Struct J 2005;102(5):745–52.
[20] Toutanji HA, Gomez W. Durability characteristics of concrete beams externally bonded with FRP composite sheets. Cement Concrete Compos 1997;19:351–8.
[21] Miyano Y, Nakada M, Sekine N. Accelerated testing for long-term durability of GFRP laminates for marine use. Compos Part B 2005;35:497–502.
[22] Chajes MJ, Thomson TA, Farschman CA. Durability of concrete beams externally reinforced with composite fabrics. Constr Build Mater 1995;9(3):141–8.
[23] Sen R, Mullins G, Salem T. Durability of E-glass/vinylester reinforcement in alkaline solution. ACI Struct J 2002;99(3):369–75.
[24] ACI 440. Guide for the design and construction of concrete reinforced with FRP bars. ACI 440.1R-01. 2001.
[25] IS: 456. Code of practice for plain and reinforced concrete. New Delhi: Bureau of Indian Standards; 1978.
[26] Neville AM. Properties of concrete. Essex, England: Pearson Education Asia Pvt. Ltd.; 2000, ISBN 981-4053-56-2.
[27] ASTM C 496-90. Test for splitting tensile strength of cylindrical concrete specimens.
[28] BS 1881: Part 117: Method for determination of tensile splitting strength. 1983.
[29] Nilson AH. Design of concrete structures. New York: McGraw-Hill; 1986.
[30] ASTM D 3039-93. Test method for tensile properties of fibre resin composites.